Mechanistic description of population dynamics using dynamic energy budget theory incorporated into integral projection models

Smallegange, I.M.; Caswell, H.; Toorians, M.E.M.; de Roos, A.M.

DOI
10.1111/2041-210X.12675

Publication date
2017

Document Version
Final published version

Published in
Methods in Ecology and Evolution

Methods in Ecology and Evolution

British Ecological Society

Methods in Ecology and Evolution 2016 doi: 10.1111/2041-210X.12675

Mechanistic description of population dynamics using dynamic energy budget theory incorporated into integral projection models

Isabel M. Smallegange*, Hal Caswell, Marjolein E. M. Toorians and André M. de Roos

Institute for Biodiversity and Ecosystem Dynamics, University of Amsterdam, PO Box 94248, Amsterdam 1090 GE, The Netherlands

Summary

1. Integral projection models (IPMs) provide a powerful approach to investigate ecological and rapid evolutionary change in quantitative life-history characteristics and population dynamics. IPMs are constructed from functions that describe the demographic rates – survival, growth and reproduction – in relation to the characteristics of individuals and their environment. Currently, however, demographic rates are estimated using phenomenological regression models that lack a mechanistic representation of the biological processes that give rise to observed demographic variation. This lack of mechanistic underpinning limits the ability of the model to predict future dynamics under novel environmental conditions because the model ingredients pertain to current environmental conditions only.

2. Here, we use dynamic energy budget (DEB) theory to construct DEB-IPMs based on a mechanistic representation of individual life-history trajectories. We derive the demographic functions describing growth and reproduction from a simple DEB growth model. The functions describing mortality and the association between parent and offspring characteristics do not follow DEB theory and hence are estimated from individual-level observations.

3. We apply the DEB-IPM to two contrasting systems: the small, fast-reproducing bulb mite *Rhizoglyphus robini* and the large, slow-reproducing reef manta ray *Manta alfredi*. In both cases, predictions of population growth rate, lifetime reproductive success and generation time agree with empirical observations. In case of the bulb mite, predictions and observations even agree across different feeding conditions.

4. If the DEB energetics model is accepted as describing growth and reproduction, DEB-IPMs can be parameterised using easy-to-collect life cycle information (growth rate, length at birth, maturation and old age) making them suitable for data-deficient species. Because species differ only in these DEB parameters, comparative studies of character and population dynamics between species are straightforward, particularly since DEB-IPMs can be extended to include population feedback on resources, of which we give an example. Most crucially, because DEB theory specifies growth and reproduction rates as explicitly dependent on environmental conditions such as food availability or temperature, DEB-IPMs provide a mechanistic platform to investigate the biological processes that determine joint change in phenotypic characters, life-history traits, population size and community structure.

Key-words: add-my-pet, cohort generation time, competition, consumer-resource dynamics, vital rates, von Bertalanffy growth rate, κ-rule growth model

Introduction

Biologists increasingly face the challenge of accurately predicting how individuals, populations and communities respond to the ever greater changes in the environment. One way of tackling this challenge is to use an approach based on the characteristics of individuals and examine how the environment affects the change of individuals in these characteristics, thereby generating the dynamics of population structure (Webb *et al.* 2010). Different types of such approaches exist, including physiologically structured population models (PSPMs; Metz & Diekmann 1986), delay-differential equation models (Nisbet & Gurney 2003), individual-based models (IBMs; Grimm & Railsback 2005), Matrix Population Models (MPMs; Caswell 2001), and Integral Projection Models (IPMs) (Easterling, Ellner & Dixon 2000). These approaches differ less in conceptual structure than in their mathematical details. MPMs and IPMs are closely and easily linked to data, but, whereas MPMs assume that individuals occupy discrete stages, IPMs accommodate both discrete and continuous state variables (e.g. Smallegange, Deere & Coulson 2014). IPMs have emerged as a powerful tool to investigate population-level processes from an

*Correspondence author. E-mail: i.smallegange@uva.nl

individual-level perspective, partly because the demographic processes of growth, survival and reproduction are estimated using flexible and easy-to-use phenomenological methods such as regression models (Ellner, Childs & Rees 2016). The downside of these regression models, however, is that they lack a mechanistic representation of the biological processes that give rise to observed survival, growth and reproduction. In this article, we discuss an alternative, more mechanistic approach to parameterisation, which explicitly incorporates an energetic description of growth and reproduction into IPMs. This will allow researchers who are not comfortable using the more mathematically challenging PSPMs, to investigate ecological and evolutionary patterns such as population dynamics, geographic distributions or evolution of life-history strategies, from an energy budget perspective on demographic rates, which has traditionally been tackled by using the mathematically more challenging PSPMs.

The character that is most commonly used to describe individuals in IPMs is body size (Ellner, Childs & Rees 2016). However, body size is determined by the process of growth, which is critically affected by food availability: the more energy is allocated to growth, the less will be available to allocate to other processes such as reproduction. When estimating demographic rates for growth and reproduction using phenomenological models, these processes are modelled independently from each other so that the latter trade-off (and hence the principle of energy conservation) is ignored. Because of the central importance of growth to any model structured by body size, it is attractive to base the model on a mechanistic representation of the individual energy budget. Dynamic energy budget (DEB) theory (Kooijman 2000) provides a well-tested framework for modelling the acquisition and use of energy for organisms during the entire life cycle. DEB models have mainly been incorporated as mechanisms in PSPMs to study density-dependent feedback effects between a population and its environment, and resulting patterns of life-history evolution (de Roos & Persson 2013). However, the analysis of PSPMs requires rather complicated methodology and PSPMs typically are more mathematical representations of biological systems. In contrast, IPMs are data-driven, provide a way of synthesising complex life-history information and can be analysed using more straightforward mathematical techniques (Smallegange & Coulson 2013). What is more, work is in progress to develop a more general approach for computing dynamic properties of nonlinear IPMs (Day & Kalies 2013). This means that, in the near future, as with PSPMs, it should be possible to analyse complex dynamics, for example by conducting bifurcation analyses of attractors (Ellner, Childs & Rees 2016).

Here, we use a simple version of the standard model of Kooijman's DEB theory, also known as the Kooijman–Metz model (Kooijman & Metz 1984), to derive the demographic functions that describe growth and reproduction. We parameterise the resulting DEB-IPM for two species that are opposites in terms of body size and life-history speed: the small, fast-reproducing bulb mite *Rhizoglyphus robini* and the large, slow-reproducing reef manta ray *Manta alfredi*. We use the parameterised DEB-IPMs to examine for mites and rays how population growth rate, lifetime reproductive success and generation time vary with feeding conditions, and assess model performance by comparing the resulting predictions against empirical observations.

Materials and methods

GENERAL STRUCTURE OF THE DEB-IPM

The DEB-IPM, like any IPM, describes the dynamics of the length number distribution $N(L, t)$ from time t to $t + 1$, with N as the number of females, by:

$$N(L',t+1)=\int_{\Omega}[D(L',L(t))R(L(t))+G(L',L(t))S(L(t))]N(L,t)\mathrm{d}L, \quad \text{eqn 1}$$

where the survival function $S(L(t))$ is the probability that an individual of length L survives from time t to $t + 1$, and $G(L', L(t))$ is the probability that an individual of length L at time t grows to length L' at $t + 1$, conditional on survival. The reproduction function $R(L(t))$ gives the number of offspring produced between time t and $t + 1$ by an individual of length L at time t. The probability density function $D(L', L(t))$ gives the probability that the offspring of an individual of length L are of length L' at time $t + 1$, and hence describes the association between parent and offspring character values. The closed interval Ω denotes the length domain. The Kooijman–Metz model is a model for the energy allocation and growth of an individual. It implies a structure for the functions $G(L', L(t))$ and $R(L(t))$; when those functions are incorporated into the IPM, the resulting model describes the dynamics of a population of individuals, each of which follows the energy budget model. Below we describe how we derive the functions $G(L', L(t))$ and $R(L(t))$ from the Kooijman–Metz model. DEB theory does not describe the rates $S(L(t))$ and $D(L', L(t))$. Parameterisation of these remaining parts of the DEB-IPM therefore in principle proceeds as in the standard IPMs, namely through regression analysis of data on survival and offspring size as a function of (parent) body size.

Growth

We assume that an individual consumes a food resource X following a scaled Holling type II functional response (Kooijman 2000), which we indicate with Y. The constant quantity Y is also referred to as the experienced feeding level as it indicates the feeding rate as a fraction of the maximum feeding rate of an individual of a particular size, ranging from zero (no feeding when $X = 0$) to one (when feeding rate equals maximum feeding rate at very high levels of X). There is no population feedback on the resource (the Supporting Information contains an example consumer-resource DEB-IPM showing how feedback between consumers and resource could be included). The Kooijman–Metz model assumes that individual organisms are isomorphic (body surface area and volume are proportional to squared and cubed length, respectively). The rate at which individuals ingest food, I, is assumed to be proportional to the maximum ingestion rate $I_{\max}$, the current feeding level Y and body surface area, and hence to the squared length of an organism: $I = I_{\max} Y L^2$. Ingested food is assimilated with a constant efficiency ε. A constant fraction κ of assimilated energy is allocated to respiration; this respiration energy equals $\kappa\varepsilon I_{\max} Y L^2$ and is used to first cover maintenance costs, which are proportional to body volume following ξL^3 (ξ is the proportionality constant relating maintenance energy requirements to cubed length), while the remainder is allocated to somatic growth. The remaining fraction $1 - \kappa$ of assimilated energy,

the reproduction energy, is allocated to reproduction in case of adults and to the development of reproductive organs in case of juveniles, and equals $(1 - \kappa)\varepsilon I_{\max} Y L^2$. From the above, the change in length L over time can be derived as (Kooijman & Metz 1984; Supporting Information):

$$\frac{\mathrm{d}L}{\mathrm{d}t} = \dot{r}_\mathrm{B}(L_\mathrm{m} \cdot Y - L), \qquad \text{eqn 2}$$

where $\dot{r}_\mathrm{B}$ is known as the von Bertalanffy growth rate and $L_\mathrm{m} = \kappa\varepsilon I_{\max}/\xi$ is the maximum length under conditions of unlimited resource. Both κ and $I_{\max}$ are assumed to be constant across experienced feeding levels, and therefore, L_m is also assumed constant. Integrating the differential eqn 2 from time t to $t + 1$ results in the function describing length at time $t + 1$ as a function of length at time t for a single individual (Supporting Information):

$$L(t+1) = L(t)\mathrm{e}^{-\dot{r}_\mathrm{B}} + (1 - \mathrm{e}^{-\dot{r}_\mathrm{B}})L_\mathrm{m} \cdot Y. \qquad \text{eqn 3}$$

Underlying eqn 3 is the assumption that growth in body length is negative, that is $L(t + 1) < L(t)$ and individuals shrink, when maintenance requirement exceed respiration energy; that is when $\xi L^3 > \kappa\varepsilon I_{\max} Y L^2$, which occurs when $L > \kappa\varepsilon I_{\max}/\xi \cdot Y \Rightarrow L > L_\mathrm{m} \cdot Y$. Shrinking in response to starvation conditions occurs in many soft-bodied invertebrates and even in vertebrates (Wikelski & Thom 2000). If organisms do not shrink under starvation conditions, additional conditions are required for eqn 3 to incorporate the mechanism that, to avoid shrinking, individuals rechannel energy from reproduction to maintenance (Supporting Information):

$$L(t+1) = \begin{cases} L(t)e^{-\dot{r}_\mathrm{B}} + (1 - e^{-\dot{r}_\mathrm{B}})L_\mathrm{m} \cdot Y & \text{for } L \le L_\mathrm{m} Y \\ L(t) & \text{otherwise.} \end{cases} \qquad \text{eqn 4}$$

Individuals die from starvation at a length at which maintenance requirements exceed the total amount of assimilated energy, that is the sum of respiration and reproduction energy: $\xi L^3 > \kappa\varepsilon I_{\max} Y L^2 + (1 - \kappa) \cdot \varepsilon I_{\max} Y L^2$, which occurs when $L > \varepsilon I_{\max}/\xi \cdot Y \Rightarrow L > L_\mathrm{m} \cdot Y/\kappa$.

Introducing interindividual variability in feeding: stochastic growth

Growth of individuals as described by eqns 3 and 4 is deterministic; for example, two individuals born at the same size will be of identical size throughout their life. Implicitly underlying the population-level model of eqn 1, however, is a stochastic, IBM, in which individuals follow Markovian growth trajectories that depend on an individual's current state (Easterling, Ellner & Dixon 2000). This individual variability is in standard IPMs modelled using a probability distribution, typically Gaussian, where the mean length and variability (model residuals) are regression functions of length (Easterling, Ellner & Dixon 2000). Parameterizing such a distribution requires an extensive data set containing pairs of body lengths measured on the same individual at time t and $t + 1$. As we aim for users to be able to also apply the DEB-IPM to data-deficient species, we take a data-independent approach. We introduce variability as arising from how individuals experience the environment. We assume that the experienced feeding level Y follows a probability distribution $f(Y)$, which means that individuals within a cohort of length L do not necessarily experience the same feeding level due to demographic stochasticity (e.g. individuals, independently of each other, have good or bad luck in their feeding experience). The expectation of this probability distribution is related to the resource density in the environment: $E(Y) = X/(K + X)$ where X represents the resource density in the environment and K is the half-saturation constant. Because the growth rate of an individual is a linear function of its experienced feeding level Y (eqn 3), our assumptions about the interindividual variability in experienced feeding level imply that the growth realised by a cohort of individuals with length $L(t)$ equals (assuming individuals can shrink):

$$\begin{aligned} E(L(t+1)) &= \int [L(t)\mathrm{e}^{-\dot{r}_\mathrm{B}} + (1 - \mathrm{e}^{-\dot{r}_\mathrm{B}})L_\mathrm{m} \cdot Y] \cdot f(Y)\mathrm{d}Y \\ &= L(t)\mathrm{e}^{-\dot{r}_\mathrm{B}} + (1 - \mathrm{e}^{-\dot{r}_\mathrm{B}})L_\mathrm{m} \int Yf(Y)\mathrm{d}Y \\ &= L(t)\mathrm{e}^{-\dot{r}_\mathrm{B}} + (1 - \mathrm{e}^{-\dot{r}_\mathrm{B}})L_\mathrm{m} \cdot E(Y). \end{aligned} \qquad \text{eqn 5}$$

The variance in length at time $t + 1$ for a cohort of individuals of length L is then given by:

$$\sigma^2(L(t+1)) = (1 - \mathrm{e}^{-\dot{r}_\mathrm{B}})^2 L_\mathrm{m}^2 \sigma^2(Y). \qquad \text{eqn 6}$$

If individuals cannot shrink, eqn 5 and eqn 6, respectively, become (Supporting Information):

$$E(L(t+1)) = \begin{cases} L(t)\mathrm{e}^{-\dot{r}_\mathrm{B}} + (1 - \mathrm{e}^{-\dot{r}_\mathrm{B}})L_\mathrm{m} \cdot E(Y) & \text{for } L \le L_\mathrm{m} E(Y) \\ L(t) & \text{otherwise,} \end{cases} \qquad \text{eqn 7}$$

and

$$\sigma^2(L(t+1)) = \begin{cases} (1 - \mathrm{e}^{-\dot{r}_\mathrm{B}})^2 L_\mathrm{m}^2 \sigma^2(Y) & \text{for } L \le L_\mathrm{m} E(Y) \\ 0 & \text{otherwise.} \end{cases} \qquad \text{eqn 8}$$

We assume that the experienced feeding level Y follows a Gaussian distribution with mean $E(Y) = X/(K + X)$ and standard deviation $\sigma(Y)$, which means that the probability density function describing growth equals:

$$G(L', L(t)) = \frac{1}{\sqrt{2\pi}\sigma_L(L(t+1))} \mathrm{e}^{\frac{-(L' - E(L(t+1)))^2}{2\sigma_L^2(L(t+1))}}, \qquad \text{eqn 9}$$

where $E(L(t + 1))$ is given by eqn 5 and $\sigma_L^2(L(t+1))$ by eqn 6 for individuals that can shrink, and by eqn 7 and eqn 8, respectively, for individuals that do not shrink under starvation conditions. Following standard practice in the construction of IPMs (Ellner, Childs & Rees 2016), eqn 9 describes a Gaussian probability distribution of body lengths at time $t + 1$ for any given body length at time t. In standard IPMs, statistical regression functions are used to estimate $E(L(t + 1))$ and $\sigma_L^2(L(t + 1))$.

Reproduction

According to the Kooijman–Metz model, reproduction, that is the number of offspring produced by an individual between time t and $t + 1$, equals $Y \cdot R_\mathrm{m} \cdot L^2/L_\mathrm{m}^2$ (Supporting Information). The parameter R_m is the maximum reproduction rate of an individual of maximum length L_m. Note that R_m is proportional to $(1 - \kappa)$ (Supporting Information), whereas L_m is proportional to κ, which controls energy conservation. However, the role of κ in the DEB-IPM is mostly implicit, as κ is used as input parameter only in the starvation condition $L > L_\mathrm{m} E(Y)/\kappa$, whereas R_m and L_m are measured directly from data. Like L_m, R_m is also proportional to $I_{\max}$ (Supporting Information); as both κ and $I_{\max}$ are assumed to be constant across experienced feeding levels, R_m is also assumed constant. Individuals are mature when they reach puberty at length L_p and only surviving adults reproduce; thus, only individuals within a cohort of length $L_\mathrm{p} \le L \le L_\mathrm{m} Y/\kappa$ reproduce. As with the growth rate, the reproduction rate of an individual is a linear function of its experienced feeding level Y with proportionality constant $R_\mathrm{m} \cdot L^2/L_\mathrm{m}^2$. Hence, the reproduction realised by a cohort of individuals of length L between time t and $t + 1$ that can shrink under starvation conditions equals:

$$R(L(t)) = \begin{cases} 0 & \text{for } L_b \le L < L_p \\ E(Y) R_m L(t)^2 / L_m^2 & \text{for } L_p \le L < L_m E(Y)/\kappa. \end{cases} \quad \text{eqn 10}$$

If individuals do not shrink under starvation conditions, eqn 10 becomes (Supporting Information):

$$R(L(t)) = \begin{cases} 0 & \text{for } L_b \le L < L_p \\ E(Y) R_m L(t)^2 / L_m^2 & \text{for } L_p \le L \le L_m E(Y) \\ \frac{R_m}{1-\kappa}\left[E(Y) L(t)^2 - \frac{\kappa L(t)^3}{L_m}\right] & \text{for } L_m E(Y) < L \le L_m E(Y)/\kappa. \end{cases} \quad \text{eqn 11}$$

Survival

For simplicity, we assume a constant, size-independent background mortality rate μ. Additionally, an individual can only survive if it is able to cover its maintenance costs (i.e. when $L \le L_m Y/\kappa$). Assuming large numbers of individuals of length L, the fraction of individuals in a cohort of length L that survive from time t to $t + 1$ equals:

$$S(L(t)) = \begin{cases} e^{-\mu} & \text{for } L \le L_m E(Y)/\kappa \\ 0 & \text{otherwise.} \end{cases} \quad \text{eqn 12}$$

If DEB-IPM users prefer to model survival size dependent, one could use a logit function (because individuals either survive or die) to regress survival data against body length so that eqn 12 becomes:

$$S(L,(t)) = \begin{cases} \frac{1}{1+e^{a+bL(t)}} & \text{for } L \le L_m E(X)/\kappa \\ 0 & \text{otherwise,} \end{cases}$$

where a and b, respectively, are the intercept and slope of the logit function.

Parent–offspring association

The same rationale that we used to construct the growth function $G(L', L(t))$ (eqn 9) is used to construct the function $D(L', L(t))$:

$$D(L', L(t)) = \begin{cases} 0 & \text{for } L < L_p \\ \frac{1}{\sqrt{2\pi\sigma_{L_b}(L(t))}} e^{\frac{-(L' - E_{L_b}(L(t)))^2}{2\sigma^2_{L_b}(L(t))}} & \text{otherwise,} \end{cases} \quad \text{eqn 13}$$

where $E_{L_b}(L(t))$ is the expected size of offspring produced by a cohort of individuals with length $L(t)$, and $\sigma^2_{L_b}(L(t))$ the associated variance. Here, for simplicity, we set $E_{L_b}(L(t))$ constant and $\sigma^2_{L_b}(L(t)) = 0$ (see below). Users that wish to relate $E_{L_b}(L(t))$ to, for example, parental body length could adopt the standard IPM approach and regress offspring body length at time $t + 1$ against parental body length at time t to obtain $E_{L_b}(L(t))$, and the associated variance, $\sigma^2_{L_b}(L(t))$, from the squared residuals (Easterling, Ellner & Dixon 2000).

PARAMETERISATION AND MODEL PERFORMANCE

Our two applications below illustrate how the DEB-IPM can be parameterised for a data-rich species (bulb mite) and data-poor species (reef manta ray). Importantly, if users do not have access to data to estimate all DEB parameters for their study species, one could check the add-my-pet data collection (Add-my-pet 2016), which contains DEB parameter estimates for >300 species, and use estimates of (closely) related species.

Parameterisation for the bulb mite

Bulb mites (Acaridae) live in the soil and feed on bulbs and tubers and are pests of many crops and ornamentals (Díaz *et al.* 2000). Bulb mites are small (100–1000 μm) and live for up to a few months. From egg to adult, they go through a larval and two to three nymph stages, which takes between 11 and 40 days depending on food quality (Smallegange 2011). To parameterise the DEB-IPM, we use data on female bulb mite life-history trajectories observed at a low (ad lib access to filter paper), and high (ad lib access to yeast), feeding-level diet (Smallegange 2011). We assume that bulb mites can shrink in response to starvation [note that model output in case of the bulb mites does not differ between whether individuals can shrink or not (Fig. S1)]. Egg length at birth is independent of feeding level and maternal length (Smallegange, Deere & Coulson 2014); hence, we set $E_{L_b}(L(t)) = L_b$ =0·166 mm (Table 1), and $\sigma^2_{L_b}(L(t)) = 0$. The maximum length observed for an adult female is L_m = 1·008 mm (Table 1). Reproduction of this female was not measured and, instead, we estimated R_m by taking the maximum, observed average daily egg production rate of adult females on the high feeding level, which equals R_m = 32 (Supporting Information). Ultimate length L_∞ is the asymptote of the von Bertalanffy growth curve in length and represents the largest length an individual can achieve at a particular feeding level. The length of the largest individual observed at the low feeding level equalled 0·642 mm, and hence, we set L_∞ = 0·642 mm (Table 1). The length of the largest individual observed on the high feeding level equalled 1·008 mm, and hence, $L_\infty = L_m$ = 1·008 mm (Table 1). Length at puberty, L_p, within species is not affected by growth and maturation rate in the Kooijman–Metz growth model (even if these vary depending on food conditions). However, bulb mites are very plastic in their size at maturity in response to food conditions (Table 1). We therefore chose to relate L_p to L_∞ using the linear relationship (Kooijman 2000, p. 270):

$$L_p = dL_\infty. \quad \text{eqn 14}$$

We took the observed L_p and L_∞ values for both feeding levels (Table 1) and, using linear least-squares regression, estimated d = 0·539 [95% confidence interval (CI): 0·134–0·945]. The basic Kooijman–Metz model assumes a constant value for $\dot{r}_B$, which, here, results in poor predictions on mite body growth and the population biology descriptors (Figs S1 and S2). Because mites show very plastic growth in response to different feeding levels (Fig. S1), we stepped away from this assumption and used a statistical approach where we linearly related $\dot{r}_B$ to feeding level and ultimate length following:

$$\dot{r}_B = 1/(\beta + \alpha L_\infty), \quad \text{eqn 15}$$

where the coefficient α and β are related to parameters from the full, scaled standard DEB model: energy conductance (α) and somatic maintenance (β) (Kooijman *et al.* 2008). To estimate α and β, we first estimated $\dot{r}_B$ for each feeding level using a nonlinear least-squares estimation procedure in R (nls function) (R Development Core Team 2013) to fit the equation $L_t = L_\infty - [L_\infty - L_b]e^{-\dot{r}_B t}$ for $\dot{r}_B$ (see also eqn 2) against observed growth curves (Smallegange 2011), with L_b and L_∞ fixed at the values observed for each feeding level (Table 1). We estimated $\dot{r}_B$ at 0·083 ± 0·001 SE (t = 74·67, $P < 0·001$) and 0·016 ± 0·0003 SE (t = 42·36, $P < 0·001$) for the high and low feeding levels, respectively. These values, along with the observed values for L_∞ for each feeding level (Table 1), were next used in a linear least-squares regression to estimate α = −137·8 and β = 151·0 [R^2 = 1·00 (no variation)] (eqn 15; Supporting Information). Mortality rate μ was set constant (eqn 12), which is for the most part justified as, in juveniles, mortality is unrelated to body length and only limitedly affected by food quality, although mortality varies with body length and food quality in adults (Smallegange, Deere & Coulson 2014). Using observed female mortality rates (per day) [coded 0 (alive) or 1 (dead)], we estimated μ = 0·02 day^{-1} (95% CI: 0·01–0·03) and μ = 0·04 day^{-1} (95% CI: 0·03–0·05) for the high and low feeding levels, respectively,

Table 1. Dynamic energy budget (DEB) parameters for female bulb mites raised individually at low and high feeding levels (Smallegange 2011), and for female reef manta rays in a population of Yaeyama Islands, Japan (Kashiwagi 2014)

		Bulb mite			Reef manta ray	
Symbol	Description	Value		Unit	Value	Unit
$E(Y)$	Expected feeding level at which DEB parameters are measured	0·64	0·95	–	NA	–
L_b	Body length at birth	0·167	0·166	mm	130	cm
L_p	Body length at puberty (maturity)	0·314	0·564	mm	380	cm
L_∞	Ultimate length	0·642	1·008	mm	NA	cm
L_m	Maximum length at $E(Y) = 1$	–	1·008	mm	550	cm
R_m	Maximum reproduction rate at L_m	–	32	# day^{-1}	1	# year^{-1}
$\dot{r}_B$	von Bertalanffy growth rate	0·016	0·083	day^{-1}	0·18	year^{-1}
κ	Energy allocation fraction to somatic maintenance and growth	0·082	0·082	–	0·80	–
μ	Mortality rate	0·03	0·03	day^{-1}	0·05	year^{-1}
$\sigma(Y)$	Standard deviation of expected feeding level used in simulations	0·1; 0·3; 0·5		–	0·1; 0·3; 0·5	–

NA, not available.

using a generalised linear mixed model with a logit function, mite identity as a random factor and a binomial error structure. We assumed an intermediate mortality rate of 0·03 day^{-1}. Finally, in the starvation condition, we set $\kappa = 0{\cdot}082$ [estimated using published data (Smallegange 2011) and standard procedures described in Add-my-pet (2016)]. All data and statistical models (fitted in R; R Development Core Team, 2013) used to estimate α, β, d, $\dot{r}_B$, R_m, μ and κ are given in the Supporting Information.

Expected feeding level $E(Y)$ ranges from zero (empty gut) to one (full gut). Here, mites on the high feeding level can be assumed to always have a full gut so that $E(Y) = 1$. However, we set $E(Y) = 0{\cdot}95$ for the high feeding level as $\sigma(Y) > 0$. Assuming that resource density is constant, expected feeding level can be related to ultimate physical length (L_∞): $E(Y) = L_\infty/L_m$ (Kooijman *et al.* 2008) so that, for the low feeding level, $E(Y) = 0{\cdot}642$ mm/1·008 mm = 0·64. We have no knowledge on $\sigma(Y)$ and therefore ran each analysis for three values of σ(Y): 0·1, 0·3 and 0·5. This does create an inconsistency as $0 \leq E(Y) \leq 1$, whereas $\sigma(Y)$ can be as high as 0·5. However, we explored these high values of $\sigma(Y)$ as (very) low values did not affect model output. Future work with probability distributions that strictly confine the experienced feeding level Y between 0 and 1 should reveal the implications of this inconsistency for model predictions.

Parameterisation for the reef manta ray

The reef manta ray (Mobulidae) is one of the largest rays in the world and is distributed world-wide in tropical and subtropical waters. They are non-migratory and live close to coasts, reefs or islands, where they aggregate at cleaning stations and areas where they feed on zooplankton (Marshall *et al.* 2011a). We chose to use the DEB-IPM with the additional assumption that individuals cannot shrink under starvation conditions (as shrinking is less likely to occur in vertebrates than in invertebrates). We use published life-history data on female reef manta rays obtained from a stable population off the coasts of Yaeyama Islands, Japan, which population growth rate is estimated at $\lambda = 1{\cdot}02$–1·03 (Kashiwagi 2014). We use the disc width, that is the distance between the two pectoral fin tips, as the measure for body length. Length at birth is measured at 130 cm and females mature at about 10 years of age at a minimum length of 380 cm (Kashiwagi 2014) and live at least 40 years, reaching a maximum length of 550 cm (Marshall, Dudgeon & Bennett 2011b). On average, adult females produce one pup every 2 years (Kashiwagi 2014), but this can be as high as one pup every year (Marshall *et al.* 2011a). Based on these observations, we set $L_b = 130$ cm, $L_p = 380$ cm, $L_m = 550$ cm and $R_m = 1$ year^{-1}. The survival rate of juveniles and adults is estimated at 0·95 year^{-1} (Kashiwagi 2014), and we set the mortality rate constant at $\mu = -\log(0{\cdot}95) = 0{\cdot}05$ year^{-1} (eqn 12). The von Bertalanffy growth rate is estimated for females at $\dot{r}_B = 0{\cdot}18$ (Kashiwagi 2014). We assumed $E_{L_b}(L(t)) = L_b = 130$ cm and $\sigma^2_{L_b}(L(t)) = 0$. For the starvation condition, we assume the commonly used value of $\kappa = 0{\cdot}80$ (Add-my-pet, 2016). Again, we explored a range of expected feeding level of $0{\cdot}65 \leq E(Y) \leq 0{\cdot}95$ for three values of $\sigma(Y)$: 0·1, 0·3 and 0·5. All data are summarised in Table 1.

Model performance

We first compared the bulb mite functions for growth and reproduction predicted for both feeding levels against independent, empirical data. We could not do test this for reef manta rays as no independent, empirical observations are available. We next used eqn 1 to create predictions of population growth rate (λ), lifetime reproductive success (R_0) and generation time (T) for each species. To this end, we discretised the IPM (eqn 1) and divided the length domain Ω into 200 very small-width discrete bins, defined as 'mesh points' (a higher number of bins did not produce different results). The result is a matrix that maps a vector of 200 size classes from time t to $t + 1$. The dominant eigenvalue of this matrix equals λ. R_0 was calculated as the dominant eigenvalue of the matrix $\mathbf{F} = \mathbf{V}(\mathbf{I} - \mathbf{GS})^{-1}$, where $\mathbf{I}$ is the identity matrix and $\mathbf{V} = \mathbf{DR}$, where $\mathbf{D}$ is a matrix that approximates the parent–offspring association kernel and $\mathbf{R}$ is a matrix that approximates the reproduction kernel (Caswell 2001). $\mathbf{G}$ and $\mathbf{S}$, respectively, are the matrix that approximates the growth function and the survival function. In the Supporting Information, we provide a detailed explanation and example of how to construct these matrices. Generation time was approximated as $T = \log(R_0)/\log(\lambda)$, which represents the time it takes a population to increase by a factor R_0 (Caswell 2001).

We used the DEB-IPM to investigate for both species the relationship between expected feeding level and the population biology descriptors λ, R_0 and T for the three values of $\sigma(Y)$ (0·1; 0·3; 0·5). In case of the mites, we compared these relationships against observed values for mites raised on the low and high feeding levels, but also on a diet of intermediate feeding level: ad lib access to oats, for which $E(Y) = L_\infty$ (oats)/L_m (yeast) = 0·857/1·008 = 0·850 (Deere, Coulson & Smallegange 2015). In case of the rays, we compared these relationships

against the estimated value of $\lambda = 1{\cdot}02$ for the Japan population (Kashiwagi 2014), the observed value of cohort generation time $T_c = 25$ years [T_c is defined as defined as the mean age at which adult reproduce and calculated, very roughly, by taking the mean of the minimum and maximum adult age: $(10 + 40)/2 = 25$ years], and $R_0 = \exp[T_c \times \log(\lambda)] = 1{\cdot}6$. Note that, for both species, we compared predicted generation time T (calculated from λ and R_0 estimated from the DEB-IPM) against observed cohort generation time T_c as no observations on T exist. However, these two measures are often similar (Caswell 2001).

Results

MODEL PERFORMANCE

It is rewarding to see that the von Bertalanffy growth function that is derived from the Kooijman–Metz DEB model fits the empirical observations on bulb mite growth well for each feeding level (Fig. 1a,b). The function describing bulb mite mean reproduction overestimates independent observations (independent because these data were not used to estimate any of the DEB parameters) on reproduction rates at the low feeding level (Fig. 1c). However, for the high feeding level, predicted mean reproduction rates match independent observations on mean bulb mite reproduction (Fig. 1d: solid and dotted lines are similar).

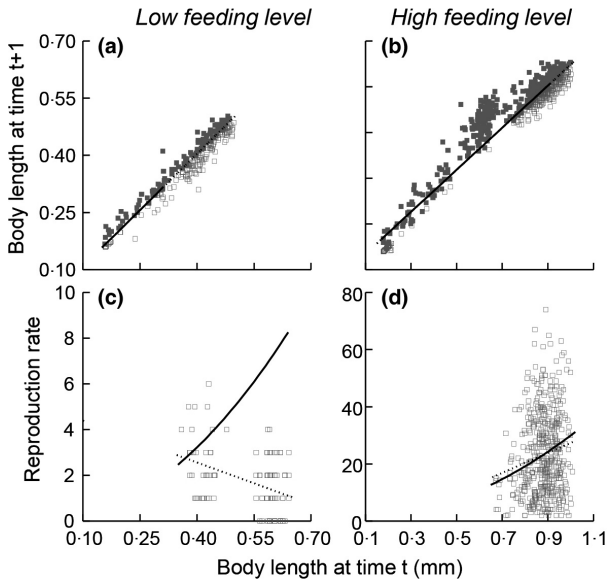

Fig. 1. Bulb mite demographic functions for growth and reproduction at time $t + 1$ in relation to body length at time t for the low and high feeding levels. Lines are predictions and symbols are observations (Smallegange 2011). In panels (a) and (b), filled symbols and solid lines, respectively, denote when observed growth and growth predicted by the dynamic energy budget-integral projection model (DEB-IPM) function for growth is greater than zero; open symbols and dotted lines, respectively, denote when observed and predicted growth is equal to or lower than zero. In panels (c) and (d), solid lines represent DEB predictions on reproduction rates, and a linear regression fit is also plotted (dotted lines) to show how mean reproduction rate relates to body length.

Unsurprisingly, both λ and R_0 increased with increasing feeding level for both bulb mites and reef manta rays (Fig. 2a–d). For the mites, predicted increases in λ and R_0 followed empirical observations (Fig. 2a,c). Even though individual reproduction rates were overestimated for large mites at $E(Y) = 0{\cdot}64$ (Fig. 1c), this did not result in an overestimation of λ at $E(Y) = 0{\cdot}64$ (Fig. 2a), but did overestimate R_0 (Fig. 2c) and thereby T (Fig. 2e) at $E(Y) = 0{\cdot}64$. Predicted R_0 at $E(Y) = 0{\cdot}95$ did not significantly differ from observed R_0 for the mites (inferred from the fact that the predicted value is within the 95% CI of the observed value) (Fig. 2c). In case of the rays, predicted λ and R_0 overlapped with observed values at feeding levels $E(Y)$ between 0·7 and 0·8 (Fig. 2b,d). Generation time for both species decreased with increasing feeding level (Fig. 2e,f). In case of the mites, only at the highest feeding level did the predicted value match observed cohort generation time T_c (Fig. 2e). In case of the rays, predicted T matched observed

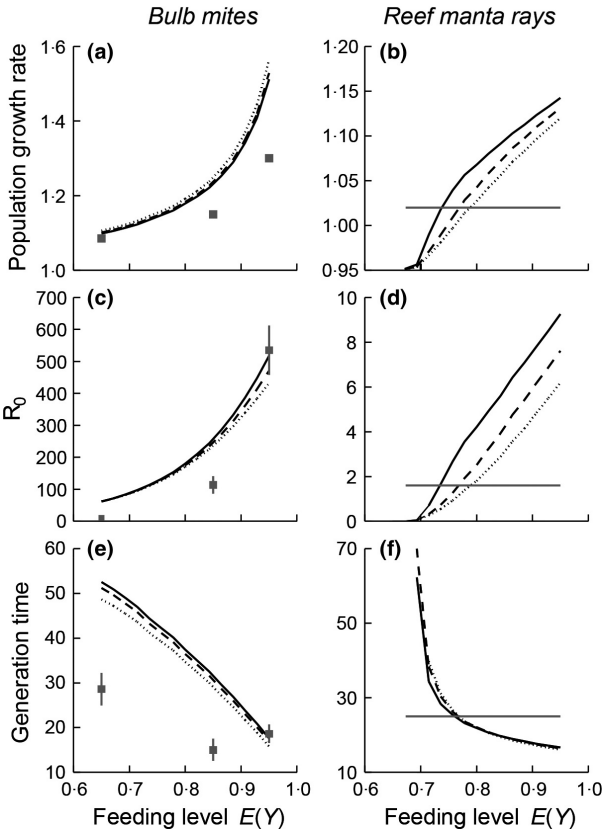

Fig. 2. Population growth rate λ [a (day^{-1}), b ($year^{-1}$)], lifetime reproductive success R_0 (c, d) and generation time T [e (days), f (years)] in relation to feeding level $E(Y)$ as predicted for three values of $\sigma(Y)$: $\sigma(Y) = 0{\cdot}1$ (solid lines); $\sigma(Y) = 0{\cdot}3$ (dashed lines) and $\sigma(Y) = 0{\cdot}5$ (dotted lines) for bulb mites (left-hand panels) and reef manta rays (right-hand panels). Grey symbols in (a), (c) and (e) are observed values for mites on low [$E(Y) = 0{\cdot}64$], intermediate [$E(Y) = 0{\cdot}85$] and high feeding levels [$E(Y) = 0{\cdot}95$]. Observed values in (a) are calculated by taking the exponent of $\log(R_0)/T_c$ (Caswell 2001), where T_c is the observed cohort generation time for bulb mites (Smallegange 2011; Deere, Coulson & Smallegange 2015). Vertical lines through the symbols in (b) and (c) are 95% CIs. Grey lines in (b), (d) and (f) are observed values for reef manta rays (Kashiwagi 2014): $\lambda = 1{\cdot}02$, $T_c = 25$ years, and $R_0 = \exp[T_c \times \log(\lambda)] = 1{\cdot}6$. See Table 1 and text for parameter values.

T_c at feeding levels of $E(Y) \approx 0{\cdot}75$ (Fig. 2f). Variation in feeding level, $\sigma(Y)$, had little effect on how each population descriptor varied with changing feeding level in case of the mites; in case of the rays, however, an increase in $\sigma(Y)$ decreased λ and R_0 across the range of explored feeding levels (Fig. 2).

Discussion

LESSONS FROM THE BULB MITE AND REEF MANTA RAY APPLICATIONS

Our application of the DEB-IPM to bulb mites and reef manta rays demonstrates the ease with which the framework can be parameterised and analysed. In case of the mites, there was a satisfactory match between predicted and observed individual growth and reproduction rates, except for reproduction by large individuals at low feeding levels. The latter mismatch was of little consequence to λ, but did result in a predicted R_0 that was much higher than what we observed. The latter discrepancy carried over to create a mismatch at the same low feeding level between observed and predicted generation times T_c and T, as T was calculated from the values of R_0 (and λ) predicted by the model. Possibly, because bulb mites are very plastic in their life-history trajectories, the assumption of a constant κ and I_{max}, and hence constant R_m and L_m (both of which are used to calculated reproduction rates), is violated. The DEB-IPM did capture the patterns of how λ, R_0 and T changed with changing feeding conditions in bulb mites, but predictions did not always fall within the CIs of data observations. To create such precise population forecasts across all feeding levels, alternative (DEB) models could be explored.

In case of the reef manta ray, we had few life-history data and no information on experienced feeding levels in the wild. However, we can glean some clues from the model output regarding experienced feeding levels. Most strikingly, values of all three predicted and observed population descriptors λ, R_0 and T each overlapped between feeding levels of 0·7–0·8; this overlap increases confidence in the model's performance. A feeding level of around 0·7–0·8 suggests that reef manta rays experience feeding levels whereby their gut is considered 'just filled', on a scale between empty and bursting (Piet & Guruge 1997). We purposefully applied the DEB-IPM to a stable population of reef manta rays, but many populations across the world are in decline, mainly due to overfishing and bycatch (Marshall *et al.* 2011a). Parameters in the DEB-IPM all have biological definitions (Table 1); an elasticity analysis targeting lower feeding levels could therefore aid in identifying which life-history processes should be prioritised in conservation research and management.

MODEL EVALUATION: STRENGTHS AND WEAKNESSES

The key strength of models based on DEBs is that they incorporate trade-offs in energy use through the κ-rule of the DEB core. This mechanistic underpinning means that the DEB-IPM is a promising tool to forecast population responses to novel or stochastically varying environmental conditions that predominantly affect growth and reproduction. To do so, using standard IPMs forces one to assume that the phenomenological demographic functions estimated for the original (constant or stationary) environment apply to individuals in the novel environment. If this assumption does not hold, for example when reproduction rates and/or size distributions differ greatly between the original and novel environment or when they vary greatly as environmental conditions vary over time, then extrapolation errors could create a substantial mismatch between predicted and actual population responses to environmental change. This is particularly likely to occur in organisms with plastic life histories; a recent stochastic, standard IPM applied to bulb mites indeed did not meet the assumption that demographic functions apply across all environments (Smallegange, Deere & Coulson 2014). A similar rationale holds for modelling density dependence under temporally varying or novel conditions. In standard IPMs, density is included as a term in the regression models describing demographic rates (Ellner, Childs & Rees 2016), again under the assumption that density dependence acts the same in the original and novel environment. Extending the DEB-IPM to include resource dynamics (one example of which is in the Supporting Information) introduces a mechanistic underpinning to density dependence that operates through resource limitation due to feedback between consumer and resource dynamics. Another strength of DEB-IPMs is that differences between species in their energy budget are mostly due to differences in their set of DEB parameters, facilitating comparative studies of character and population dynamics between species. Here, for example, we found that varying the variance in expected feeding level, $\sigma(Y)$, had little effect on predicted population growth rate and lifetime reproductive success in mites (lines in Fig. 2a,c are very similar and sometimes overlap), but did result in different values for each expected feeding level $E(Y)$ in case of the reef manta ray (lines in Fig. 2b,d are widely spaced). What drives these differences remains to be explored. Furthermore, unlike standard IPMs, no long-term individual-level data scored from birth to death are required for model parameterisation; instead, to run the DEB-IPM, one needs only seven parameter estimates (L_b, L_p, L_m, R_m, $\dot{r}_B$, κ and μ). This is of particular benefit to study systems where it is difficult to track the life history of the same individual (e.g. micro-organisms, small (soil-dwelling) animals). Even if limited or no DEB data are available, one can resort to the add-my-pet data collection and use DEB parameter estimates of related species as a starting point (Add-my-pet 2016).

For the purpose of this study, we chose to use the most simple DEB growth model, but more complex alternatives exist. For example, within the 'standard' animal DEB model (Sousa *et al.* 2010), individuals can build up reserves and use them when starving (in the Kooijman–Metz model, individuals die instantaneously when they cannot cover maintenance costs). This model has been simplified to the 'scaled standard model' (Kooijman *et al.* 2008), but the use of scaling and compound parameters hampers the interpretation of equations (Jager, Martin & Zimmer 2013). In turn, Jager, Martin &

Zimmer (2013) simplified the standard animal DEB model, mainly by not including state variables for reserve and maturity. Their resulting DEBkiss model is very similar to the Kooijman–Metz model but with the addition of an embryonic stage, a strict mass balance and direct links to metabolic processes (Jager, Martin & Zimmer 2013). However, incorporating these DEB growth models into IPMs will be challenging, given the complexity of relating body length at time $t + 1$ and at time t from the model's differential equations. Furthermore, the parent–offspring and survival functions in the DEB-IPM are not mechanistically derived. Here, we assumed that individuals suffer a background mortality and die instantaneously the moment they cannot meet their energy requirements for maintenance. In reality, individuals can survive such periods of starvation by using reserves. However, in a test of how well an individual-based DEB model that includes reserve dynamics describes population patterns, Martin *et al.* (2013) concluded that the dynamics of starvation and recovery are too poorly understood to accurately predict population fluctuations. Only by including extra assumptions on food-dependent mortality were they able to match model predictions to independent observations from population experiments. Here, we have set a first step towards developing a more mechanistic IPM based on DEB theory. Although extending our framework is complex, we emphasise that structured population models, of any mathematical form, may benefit from the incorporation of mechanisms. For example, Alver *et al.* (2016) include food, energetics and temperature dependence in a partial differential equation model for marine copepods, coupled to ocean circulation. The possibilities for inclusion of mechanism are potentially endless.

OUTLOOK: EVOLUTIONARY CHANGE

The DEB-IPM, like most IPMs, does not include genes and hence does not explicitly incorporate evolution. Simple evolutionary insight can still be obtained through the estimation of evolutionary quantities such as the strength of viability and fertility selection (Smallegange & Coulson 2013), which are calculated as the difference in population-level mean body length after and before survival, or after and before reproduction, respectively. When evolutionary change in character values takes many generations, analysis of a DEB-IPM will likely provide insight into current population, life history and character dynamics. To study long-term evolutionary change, one could apply evolutionary game theory to a DEB-IPM to study the endpoints of trait evolution (e.g. Childs *et al.* 2011), but, then, the ecological and evolutionary time-scales are decoupled. Coulson *et al.* (2016) recently developed a framework that explicitly couples evolution and ecology by linking quantitative genetics and IPMs. For systems where the rate of evolutionary change in character distributions is likely to be (fairly) close to the rate of change observed on ecological time-scales, the latter framework would be highly suited to study change in phenotypic character distributions. If, in such cases, one is interested in the ecological and evolutionary dynamics of body size and its role in population and community dynamics, one would profit from incorporating the DEB-IPM into this framework. Such an endeavour would be particularly insightful in studies that focus on the eco-evolutionary dynamics of parameters that play an important role in individual life histories, such as size at birth or at maturity. This would require a multivariate DEB-IPM where the dynamics of each of these characters is modelled alongside the dynamics of body size. The accompanying challenges in doing so, however, at the moment, makes this a distant goal.

Acknowledgements

This paper benefitted greatly from discussions with Lars Kramer and members of the Theoretical Ecology group. We thank Lars Kramer for estimating the DEB parameters of the mites. IMS is funded by a MEERVOUD grant no. 836.13.001 and VIDI grant no. 864.13.005 from the Netherlands Organisation for Scientific Research. HC is funded by an ERC Advanced Grant 322989. AMdR is supported by funding from the European Research Council under the European Union's Seventh Framework Programme (FP/2007-2013)/ERC Grant Agreement No. 322814.

Data accessibility

Uploaded as supporting information is a pdf-file explaining how to model growth and reproduction, the DEB-IPM (including a toy example) and a consumer-resource DEB-IPM. MatLab scripts to run the DEB-IPM and r-scripts and data files to estimate the bulb mite DEB parameters can be downloaded from: https://figshare.com/s/3432986aff18d8b431ee.

References

Add-my-pet (2016) Database of code, data and DEB model parameters. www.debtheory.org.

Alver, M.O., Broch, O.J., Melle, W., Bagoien, E. & Slagstad, D. (2016) Validation of an Eulerian population model for the marine copepod *Calanus finmarchicus* in the Norwegian Sea. *Journal of Marine Systems*, **160**, 81–93.

Caswell, H. (2001) *Matrix Population Models: Construction, Analysis, and Interpretation*. Sinauer Associates, Sunderland, MA, USA.

Childs, D.Z., Coulson, T.N., Pemberton, J.M., Clutton-Brock, T.H. & Rees, M. (2011) Predicting trait values and measuring selection in complex life histories: reproductive allocation decisions in Soay sheep. *Ecology Letters*, **14**, 985–992.

Coulson, T., Plard, F., Schindler, S., Ozgul, A. & Gaillard, J.-M. (2016) Quantitative genetics meets integral projection models: unification of widely used methods from ecology and evolution. arXiv:1509.01351

Day, S. & Kalies, W.D. (2013) Rigorous computation of the global dynamics of integrodifference equations with smooth nonlinearities. *Siam Journal on Numerical Analysis*, **51**, 2957–2983.

Deere, J.A., Coulson, T. & Smallegange, I.M. (2015) Life history consequences of the facultative expression of a dispersal life stage in the phoretic bulb mite (*Rhizoglyphus robini*). *PLoS One*, **10**, e0136872.

Díaz, A., Okabe, K., Eckenrode, C.J., Villani, M.G. & O'Connor, B.M. (2000) Biology, ecology, and management of the bulb mites of the genus *Rhizoglyphus* (Acari: Acaridae). *Experimental and Applied Acarology*, **24**, 85–113.

Easterling, M.R., Ellner, S.P. & Dixon, P.M. (2000) Size-specific sensitivity: applying a new structured population model. *Ecology*, **81**, 694–708.

Ellner, S.P., Childs, D.Z. & Rees, M. (2016) *Data-Driven Modelling of Structured Populations. A Practical Guide to the Integral Projection Model*. Lecture Notes on Mathematical Modelling in the Life Sciences. Springer, Cham, Switzerland.

Grimm, V. & Railsback, S.F. (2005) *Individual-Based Modeling and Ecology*. Princeton University Press, Princeton, NJ, USA.

Jager, T., Martin, B.T. & Zimmer, R.I. (2013) DEBkiss or the quest for the simplest generic model of animal life history. *Journal of Theoretical Biology*, **328**, 9–18.

Kashiwagi, T. (2014) *Conservation Biology and Genetics of the Largest Living Rays: Manta Rays*. PhD thesis. The University of Queensland, Brisbane, Qld, Australia.

Kooijman, S.A.L.M. (2000) *Dynamic Energy and Mass Budgets in Biological Systems*, 2nd edn. Cambridge University Press, Cambridge, UK.

Kooijman, S.A.L.M. & Metz, J.A.J. (1984) On the dynamics of chemically stressed populations: the deduction of population consequences from effects on individuals. *Ecotoxicology and Environmental Safety*, **8**, 254–274.

Kooijman, S.A.L.M., Sousa, T., Pecquerie, L., van der Meer, J. & Jager, T. (2008) From food-dependent statistics to metabolic parameters, a practical guide to the use of dynamic energy budget theory. *Biological Reviews*, **83**, 533–552.

Marshall, A.D., Dudgeon, C.L. & Bennett, M.B. (2011b) Size and structure of a photographically identified population of manta rays *Manta alfredi* in southern Mozambique. *Marine Biology*, **158**, 1111–1124.

Marshall, A.D., Kashiwagi, T., Bennett, M.B., Deakos, M., Stevens, G., McGregor, F., Clark, T., Ishihara, H. & Sato, K. (2011a) *Manta alfredi*. The IUCN Red List of Threatened Species Version 2015.2.

Martin, B.T., Jager, T., Nisbet, R.M., Preuss, T.G. & Volker, G. (2013) Predicting population dynamics from the properties of individuals: a cross-level test of dynamic energy budget theory. *The American Naturalist*, **181**, 506–519.

Metz, J.A.J. & Diekmann, O. (1986) *The Dynamics of Physiologically Structured Populations*. Springer, Berlin, Germany.

Nisbet, R.M. & Gurney, W.S.C. (2003) *Modelling Fluctuating Populations*. Blackburn Press, Caldwell, NJ, USA.

Piet, G.J. & Guruge, W.A.H.P. (1997) Diel variation in feeding and vertical distribution of ten co-occurring fish species: consequences for resource partitioning. *Environmental Biology of Fishes*, **50**, 293–307.

R Development Core Team (2013) *R: A Language and Environment for Statistical Computing*. R Foundation for Statistical Computing, Vienna, Austria. http://www.R-project.org/.

de Roos, A.M. & Persson, L. (2013) *Population and Community Ecology of Ontogenetic Development* (Monographs in Population Biology, 51). Princeton University Press, Princeton, NJ, USA.

Smallegange, I.M. (2011) Effects of paternal phenotype and environmental variability on age and size at maturity in a male dimorphic mite. *Naturwissenschaften*, **98**, 339–346.

Smallegange, I.M. & Coulson, T. (2013) Towards a general, population-level understanding of eco-evolutionary change. *Trends in Ecology and Evolution*, **28**, 143–148.

Smallegange, I.M., Deere, J.A. & Coulson, T. (2014) Correlative changes in life-history variables in response to environmental change in a model organism. *American Naturalist*, **183**, 784–797.

Sousa, T., Domingos, T., Poggiale, J.C. & Kooijman, S.A.L.M. (2010) Dynamic energy budget theory restores coherence in biology. *Philosophical Transactions of the Royal Society of London B: Biological Sciences*, **365**, 3413–3428.

Webb, C.T., Hoeting, J.A., Ames, G.M., Pyne, M.I. & Poff, N.L. (2010) A structured and dynamic framework to advance traits-based theory and prediction in ecology. *Ecology Letters*, **13**, 267–283.

Wikelski, M. & Thom, C. (2000) Marine iguanas shrink to survive El Niño. *Nature*, **403**, 37–38.

Received 5 August 2016; accepted 28 September 2016
Handling Editor: Jessica Metcalf

Supporting Information

Additional Supporting Information may be found online in the supporting information tab for this article:

Appendix S1. Which includes:

1 Modelling growth and reproduction from the Kooijman–Metz model.

2 Consequences of variable von Bertalanffy growth rate in mites.

3 Additional assumptions of the DEB-IPM: when individuals do not shrink.

4 Building the DEB-IPM: a detailed explanation and toy example.

5 Consumer-resource DEB-IPM: construction and a bulb mite application.